Production of the ϕ vector-meson in heavy ion collisions

Catarina Quintans for the NA50 collaboration

M.C. Abreu[6,a], B. Alessandro[10], C. Alexa[3], R. Arnaldi[10], M. Atayan[12], C. Baglin[1], A. Baldit[2], M. Bedjidian[11], S. Beolè[10], V. Boldea[3], P. Bordalo[6,b], A. Bussière[1], L. Capelli[11], L. Casagrande[6,c], J. Castor[2], T. Chambon[2], B. Chaurand[9], I. Chevrot[2], B. Cheynis[11], E. Chiavassa[10], C. Cicalò[4], T. Claudino[6], M.P. Comets[8], N. Constans[9], S. Constantinescu[3], N. De Marco[10], A. De Falco[4], G. Dellacasa[10,d], A. Devaux[2], S. Dita[3], O. Drapier[11], L. Ducroux[11], B. Espagnon[2], J. Fargeix[2], P. Force[2], M. Gallio[10], Y.K. Gavrilov[7], C. Gerschel[8], P. Giubellino[10], M.B. Golubeva[7], M. Gonin[9], A.A. Grigorian[12], J.Y. Grossiord[11], F.F. Guber[7], A. Guichard[11], H. Gulkanyan[12], R. Hakobyan[12], R. Haroutunian[11], M. Idzik[10,e], D. Jouan[8], T.L. Karavitcheva[7], L. Kluberg[9], A.B. Kurepin[7], Y. Le Bornec[8], C. Lourenço[5], P. Macciotta[4], M. Mac Cormick[8], A. Marzari-Chiesa[10], M. Masera[10], A. Masoni[4], S. Mehrabyan[12], M. Monteno[10], A. Musso[10], P. Petiau[9], A. Piccotti[10], J.R. Pizzi[11], F. Prino[10], G. Puddu[4], C. Quintans[6], S. Ramos[6,b], L. Ramello[10,d], P. Rato Mendes[6], L. Riccati[10], A. Romana[9], I. Ropotar[5], P. Saturnini[2], E. Scomparin[10] S. Serci[4], R. Shahoyan[6,f], S. Silva[6], M. Sitta[10,d], C. Soave[10], P. Sonderegger[5,b], X. Tarrago[8], N.S. Topilskaya[7], G.L. Usai[4], E. Vercellin[10], L. Villatte[8], N. Willis[8].

[1] LAPP, CNRS-IN2P3, Annecy-le-Vieux, France; [2] LPC, Univ. Blaise Pascal and CNRS-IN2P3, Aubière, France; [3] IFA, Bucharest, Romania; [4] Università di Cagliari/INFN, Cagliari, Italy; [5] CERN, Geneva, Switzerland; [6] LIP, Lisbon, Portugal; [7] INR, Moscow, Russia; [8] IPN, Univ. de Paris-Sud and CNRS-IN2P3, Orsay, France; [9] LPNHE, Ecole Polytechnique and CNRS-IN2P3, Palaiseau, France; [10] Università di Torino/INFN, Torino, Italy; [11] IPN, Univ. Claude Bernard Lyon-I and CNRS-IN2P3, Villeurbanne, France; [12] YerPhI, Yerevan, Armenia.

a) also at UCEH, Universidade de Algarve, Faro, Portugal; b) also at IST, Universidade Técnica de Lisboa, Lisbon, Portugal; c) now at CERN; d) Universitá del Piemonte Orientale, Alessandria and INFN-Torino, Italy; e) now at Faculty of Physics and Nuclear Techniques, University of Mining and Metallurgy, Cracow, Poland; f) on leave of absence of YerPhI, Yerevan, Armenia.

Abstract

Strangeness production in relativistic heavy ion collisions has been studied by experiments NA38 and NA50 (both at the CERN/SPS), through the vector-mesons ϕ and $\rho + \omega$. Results from p-W, S-S, S-Cu and S-U at 200 A GeV, and Pb-Pb at 158 A GeV are studied as a function of the dimuon transverse momentum and the collision centrality. A factor 2 enhancement of the ϕ production is observed in sulphur and lead induced reactions. A multiplicity study as a function of the number of participants is shown for Pb-Pb interactions. The power law A dependence of the inclusive cross-sections is investigated. Inverse slope parameters are obtained from the $\mathrm{d}\sigma/\mathrm{dM}_T$ spectra for the ϕ and the $\rho + \omega$ vector-mesons.

1. Introduction

It was predicted a long time ago that, if sufficiently high temperature and/or compression conditions are achieved, a phase transition from nuclear matter into a quark-gluon plasma (QGP) occurs. In this new state of matter quarks and gluons are no longer confined inside hadrons but behave as free particles. This is accompanied by a partial chiral symmetry restoration. Plasma signatures experimentally accessible include J/ψ suppression, strangeness enhancement, the ρ broadening and direct photon emission.

The overproduction of $s\bar{s}$ pairs, both due to chiral symmetry restoration and to the Pauli blocking mechanism, is a signature for the phase transition [1,2] searched by several ultra-relativistic heavy ion experiments. Experiments NA38 and NA50 study the dimuon spectra produced in such collisions and are able to detect and identify ρ, ω and ϕ mesons.

2. Experimental apparatus

The NA38 and NA50 experimental apparatus consists mainly of a muon spectrometer, an hadron absorber, an electromagnetic calorimeter, a zero degree calorimeter (only in NA50) and a beam hodoscope. The target consists of several small subtargets instrumented for individual identification of the interaction vertex.

NA38 had a special set-up for the study of the ϕ mass region. The three inner rings of the calorimeter were replaced by an Al_2O_3 absorber. A pre-absorber of the same material was added, for a better reduction of the background originating from π and K decays into muons. This set-up was used for the study of p-W, S-S, S-Cu and S-U with a 200 A GeV beam (S-S and S-Cu were short data taking periods) [3].

In the case of NA50, the experiment was optimized for J/ψ studies, with the magnetic field increased by a factor 1.75 with respect to NA38, implying that the ϕ region suffers from very low acceptance for dimuons with $M_T < 1.5$ GeV/c^2. Several detectors were added to the apparatus, namely a multiplicity detector and a zero degree calorimeter located inside the main absorber, to measure the spectators energy. The details of the apparatus used to study Pb-Pb collisions with 158 A GeV beam energy can be found in [4].

The kinematical domain used in this analysis is: dimuon mass in the range $0.25 \leq M_{\mu\mu} \leq 2.5$ GeV/c^2 ($0.25 \leq M_{\mu\mu} \leq 2.0$ GeV/c^2 for Pb-Pb); the rapidity window $0. \leq Y_{\mu\mu}^{CM} \leq 1.$; and the Collins-Soper muon angle $-0.5 \leq \cos\theta_{CS} \leq 0.5$. The dimuons transverse momentum range is $0.6 \leq p_T \leq 3.0$ GeV/c for proton and sulphur induced collisions. For Pb-Pb collisions dimuon transverse masses $1.5 \leq M_T \leq 3.2$ GeV/c^2 are studied.

The combinatorial background is estimated from the like sign muon pairs according to: $N_{bkg} = 2\sqrt{N^{++}N^{--}}$. In the ϕ mass region, one obtains ratios signal/background from 0.2 to 2.2 (depending on the p_T region studied) for S-S; 0.2 - 2.6 for S-Cu; 0.2 - 2.3 for S-U and ≈ 0.4 for Pb-Pb (integrated for $M_T \geq 1.5$ GeV/c^2).

3. Method of analysis

Muon tracks are reconstructed and vertices identified. The kinematical and quality cuts are applied, and the background subtraction is performed. The acceptance and the smearing effects are evaluated with a dedicated Monte Carlo code, using as input a generation function consisting of three classical Breit-Wigner functions and an exponential depending on the mass (an effective parametrisation of the continuum due to Drell-Yan, open-charm decays and Dalitz decays of η, $\eta\prime$ and ω's). The generated events are reconstructed as if they were real data. The extracted smearing function and acceptance are then used to correct the data.

The experimental mass spectra, corrected for acceptance and smearing effects, are fitted with a five free parameter function, accounting for all known contributions:

$$F = P_1\ BW^{\rho} + P_2\ BW^{\omega} + P_3\ BW^{\phi} + P_4\ exp(-P_5 M_{\mu\mu})$$

where we use the PDG values for the resonance masses and natural widths.

4. Cross-sections

The sulphur induced reactions are analised in 5 p_T bins. From the number of events produced in a given kinematical domain, the luminosity and all the efficiencies, one can calculate the differential resonance cross-sections in the dimuon channel (see fig. 1).

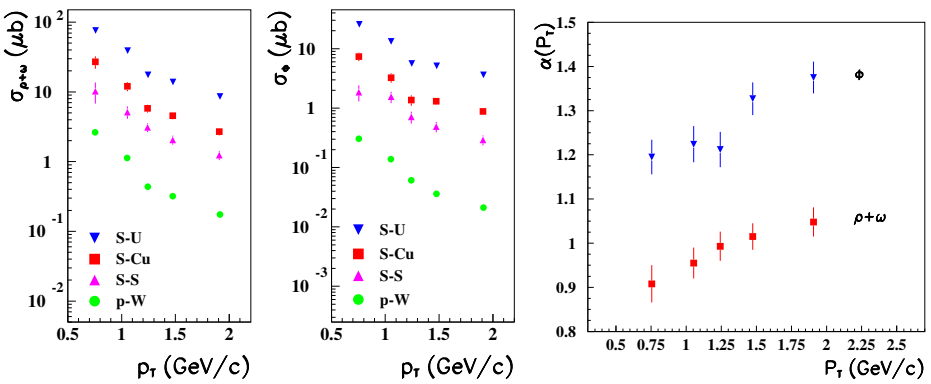

Figure 1. Differential cross-sections (per p_T region) for $\rho + \omega$ and ϕ (left) and power law A dependencies (right) for proton and sulphur induced collisions.

The target recognition algorithm efficiency depends on the centrality ($\approx 100\%$ for central events, but poor for very peripheral ones). The correction is done on an event-by-event basis, but very low E_T events are rejected, to avoid big uncertainties in this efficiency.

The power law A dependence of the cross-section is parametrized according to $\sigma = \sigma_o \, (A \cdot B)^{\alpha}$. The α parameter extracted from fits to the proton and sulphur data is: $\alpha_{\rho+\omega} = 0.927 \pm 0.034$; $\alpha_{\phi} = 1.226 \pm 0.030$. Its dependence with p_T is shown in fig. 1 (right), where the Cronin effect is visible for both resonances. There is a clear overproduction of the ϕ, as can be seen from the α_{ϕ} values bigger than unity.

5. Ratio $\phi/(\rho + \omega)$

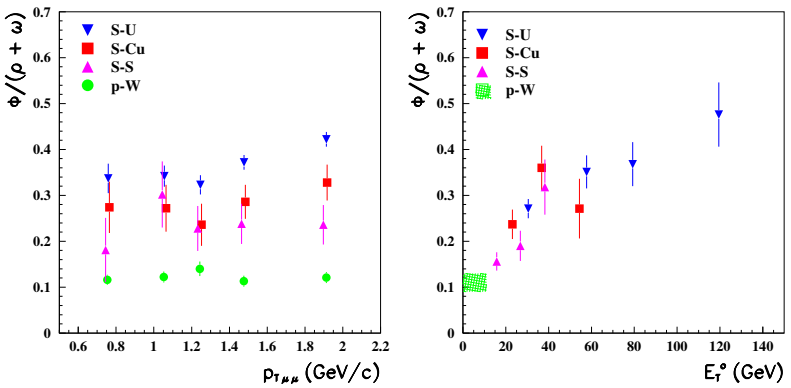

Figure 2. $\phi/(\rho + \omega)$ as a function of p_T (left) and as a function of E_T (right).

The enhancement of strangeness can also be studied through the ratio $B_{\mu\mu}\sigma_{\phi}/(B_{\mu\mu}\sigma_{\rho} + B_{\mu\mu}\sigma_{\omega})$ (abbreviated to $\phi/(\rho + \omega)$ from now on). Fig. 2 (left) shows $\phi/(\rho + \omega)$ as a function

of p_T, no dependence being seen. When this ratio is studied as a function of the collision neutral transverse energy (see fig. 2 right) a clear increase by a factor of ≈ 5 is observed when going from p-W to central S-U (S-S and S-Cu follow the same trend as the S-U data points). Within the same system, a dependence on the collision centrality is also seen.

6. Inverse Slopes

Assuming a locally equilibrated thermal radiation source, cross-sections follow an universal M_T scaling that, when resonance masses are much higher than the inverse slopes and for not too low values of p_T, can be expressed by: $\frac{d\sigma}{dM_T} \propto M_T^{3/2}\, e^{-M_T/T}$.

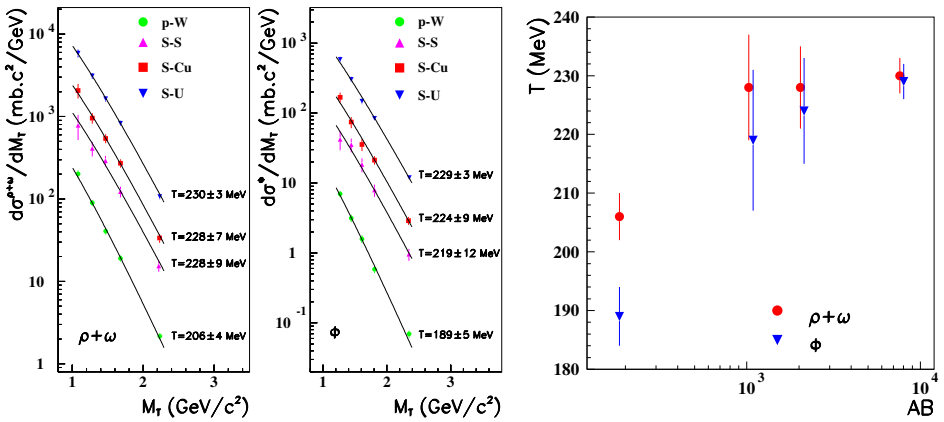

Figure 3. Transverse mass cross-sections for $\rho + \omega$ and ϕ (left) and the inverse slope parameter dependence with AB (right), for p and S induced reactions.

Fig. 3 shows the inverse slope parameters obtained for both $\rho+\omega$ and ϕ, using the above expression. Differential cross-sections were divided by the corresponding M_T bin widths, and also by the branching ratios into dimuons. Also shown is the dependence with AB of the inverse slopes. As can be seen, the inverse slopes obtained are the same for $\rho + \omega$ and for ϕ, within the error bars. Parameter T increases when going from proton to sulphur induced collisions and there seems to be a saturation within sulphur systems.

7. Pb-Pb 1996 results

We use a different method of analysis for the Pb-Pb data taken by experiment NA50 in 1996. In this method one simulates each contribution to the dimuon mass spectrum independently. While the mass distributions used for ω and for ϕ are classical Breit-Wigner functions, the much broader ρ vector-meson is parametrized with a Breit-Wigner function including the non-resonant background under the ρ. With the generated events, reconstructed as if they were real data, one obtains smeared MC functions accounting for the several contributions to the spectrum, that are then used to fit the experimental mass spectra. The fit function has five free parameters: the normalizations for $\rho + \omega$, ϕ and continuum and the mass values for ϕ and ω (more details on this method of analysis are given in [5]). About 130000 ϕ events are reconstructed from the 1996 lead data.

The ratios $\phi/(\rho + \omega)$ are studied in 5 M_T bins ($1.5 \leq M_T \leq 3.2$ GeV/c^2), and 9 E_T bins. Fig. 4 shows these ratios (acceptance corrections included). The flat trend with M_T points to a similar behaviour of the ϕ and the $\rho + \omega$ with respect to the dimuon transverse

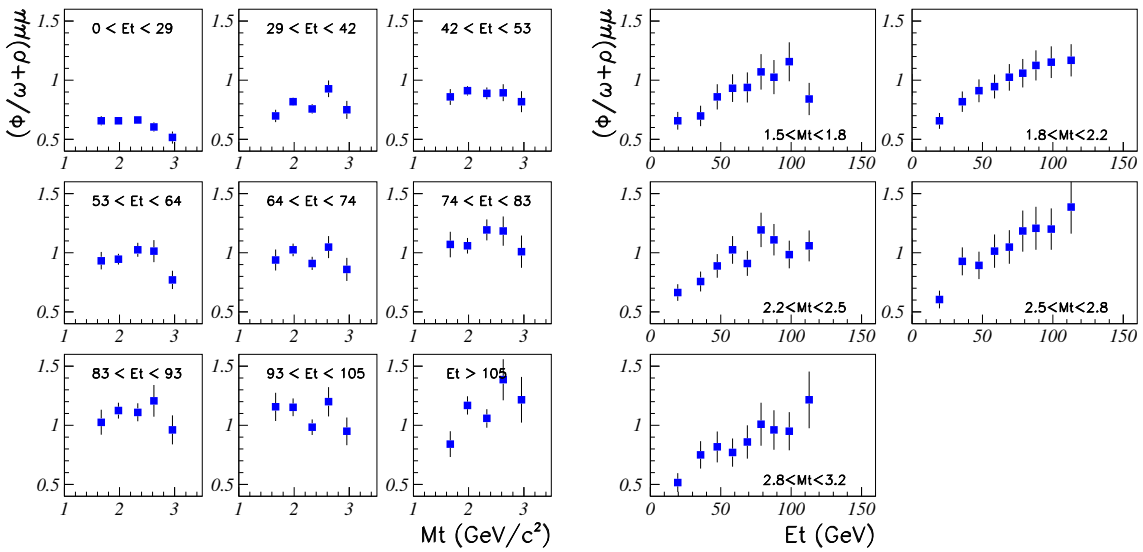

Figure 4. Ratio $\phi/(\rho+\omega)$ as a function of M_T in different E_T bins (left) and as a function of E_T in different M_T bins (right), for Pb-Pb reactions.

mass. The ratio depends clearly on the centrality of the collisions, as can be seen from each of the 5 studied M_t bins. This increase amounts to a factor 2.

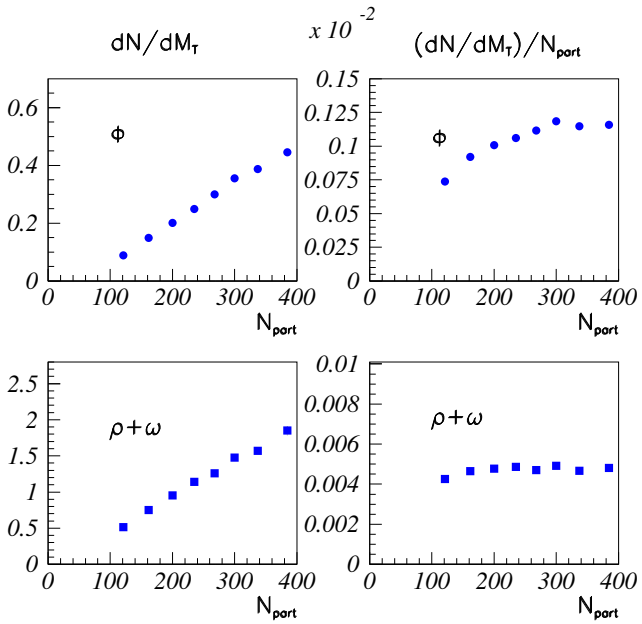

Figure 5. Multiplicities and multiplicities per participant for $\rho+\omega$ and ϕ (Pb-Pb reactions).

The resonance's multiplicity, interpreted as the number of produced particles per collision divided by the width of the M_T bin where it was evaluated, is presented in fig. 5 as a function of the number of participant nucleons in the collision, N_{part}. N_{part} is evaluated with the Glauber Model for each E_T bin, from the mean E_T value. An increase is observed for both resonances, but when dividing the multiplicities per participant $\rho + \omega$ remains constant while ϕ is enhanced for central collisions.

Fits to the M_T differential cross-section with a function $1/M_T\ d\sigma/dM_T \propto exp(-M_T/T)$ are shown in fig. 6. The inverse slope parameter values obtained are $T_{\rho+\omega} = 224 \pm 10$ MeV and $T_\phi = 227 \pm 10$ MeV. Applying the fit function $d\sigma/dM_T \propto M_T^{3/2}\ exp(-M_T/T)$ used for the sulphur systems leads to slightly lower results, $T_{\rho+\omega} = 213 \pm 10$ MeV and $T_\phi = 216 \pm 10$ MeV, but in agreement with sulphur values within error bars.

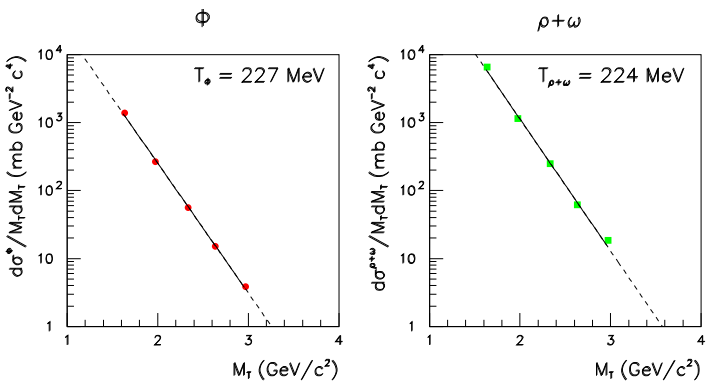

Figure 6. Inverse slope parameters for ϕ and $\rho + \omega$ (Pb-Pb reactions).

8. Conclusions

The increased production of strangeness with the energy density, predicted by QCD, was observed in heavy ion collisions as compared to proton induced collisions. The overproduction of the ϕ vector-meson is clearly observed through the A dependence of the cross-section with a power law bigger than unity. For the lead induced reactions this same conclusion is suggested by the increased ϕ multiplicity per participant with the number of participants. The ratio $\phi/(\rho + \omega)$ gives another hint on the strangeness production, showing an increase with the centrality of the collisions.

The inverse slope parameter extracted from the universal M_T scaling of the cross-sections depends both on the freeze-out temperature of the interacting system and on its collective expansion velocity. The obtained values for this T parameter increase when going from proton to sulphur induced reactions, and then seem to saturate.

References

[1] Koch P, Muller B and Rafelski J 1986 *Phys. Rep.* **142** 167
[2] Shor A 1985 *Phys. Rev.* **54** 1122
[3] Baglin C et al (NA38 Coll.) 1989 *Phys. Lett.* B **220** 471 and 1991 *Phys. Lett.* B **255** 459
[4] Abreu M C et al (NA50 Coll.) 1997 *Phys. Lett.* B **410** 327 and 1997 *Phys. Lett.* B **410** 337
[5] Villatte L for the NA50 Coll. *Proc. XXXVIII Int. Winter Meeting on Nuclear Physics* Bormio Italy January 24-29 2000